© 2014. Published by The Company of Biologists Ltd | Journal of Cell Science (2014) 127, 258 doi:10.1242/jcs.145946

CORRECTION

Rab4b controls an early endosome sorting event by interacting with the γ-subunit of the clathrin adaptor complex 1

Laura Perrin, Sandra Lacas-Gervais, Jérôme Gilleron, Franck Ceppo, François Prodon, Alexandre Benmerah, Jean-François Tanti and Mireille Cormont

There was an error published in *J. Cell Sci.* **126**, 4950–4962.

All author names were transposed and indexed under first names. The correct author list is as shown above.

We apologise to the authors and readers for any confusion that this error might have caused.

Journal of Cell Science

Rab4b controls an early endosome sorting event by interacting with the γ-subunit of the clathrin adaptor complex 1

Perrin Laura[1,2,*], Lacas-Gervais Sandra[3], Gilleron Jérôme[1,2], Ceppo Franck[1,2], Prodon François[1,2,‡], Benmerah Alexandre[4,5], Tanti Jean-François[1,2] and Cormont Mireille[1,2,§]

[1]INSERM U1065, Centre Méditerranéen de Médecine Moléculaire C3M, Nice, France
[2]Université de Nice Sophia-Antipolis, Nice, France
[3]Université de Nice Sophia-Antipolis, Centre Commun de Microscopie Appliquée CCCMA, Nice, France
[4]INSERM U983, Institut Cochin, Paris, France
[5]Université Paris Descartes, Sorbonne Paris Cité, Institut Imagine, Paris, France

*Present address: CENBG, Centre d'Etudes Nucléaires de Bordeaux Gradignan, CNRS UMR5797, Université Bordeaux 1, Gradignan, France
‡Present address: Université de Genève, Bioimaging team, Genève, Switzerland
§Author for correspondence (cormont@unice.fr)

Accepted 8 August 2013
Journal of Cell Science 126, 4950–4962

doi: 10.1242/jcs.130575

Summary

The endocytic pathway is essential for cell homeostasis and numerous small Rab GTPases are involved in its control. The endocytic trafficking step controlled by Rab4b has not been elucidated, although recent data suggested it could be important for glucose homeostasis, synaptic homeostasis or adaptive immunity. Here, we show that Rab4b is required for early endosome sorting of transferrin receptors (TfRs) to the recycling endosomes, and we identified the AP1γ subunit of the clathrin adaptor AP-1 as a Rab4b effector and key component of the machinery of early endosome sorting. We show that internalised transferrin (Tf) does not reach Vamp3/Rab11 recycling endosomes in the absence of Rab4b, whereas it is rapidly recycled back to the plasma membrane. By contrast, overexpression of Rab4b leads to the accumulation of internalised Tf within AP-1- and clathrin-coated vesicles. These vesicles are poor in early and recycling endocytic markers except for TfR and require AP1γ for their formation. Furthermore, the targeted overexpression of the Rab4b-binding domain of AP1γ to early endosome upon its fusion with FYVE domains inhibited the interaction between Rab4b and endogenous AP1γ, and perturbed Tf traffic. We thus proposed that the interaction between early endocytic Rab4b and AP1γ could allow the budding of clathrin-coated vesicles for subsequent traffic to recycling endosomes. The data also uncover a novel type of endosomes, characterised by low abundance of either early or recycling endocytic markers, which could potentially be generated in cell types that naturally express high level of Rab4b.

Key words: Rab, Rab4b effector, Endocytic recycling

Introduction

The GTPase Rab4b is phylogenetically conserved from yeast *Schizosaccharomyces pombe* (Ypt4) to metazoans. The Rab4a orthologous gene is present in Zebrafish and was conserved during evolution through metazoans. Rab4b and Rab4a are encoded by two genes. The Rab proteins were classified according to phylogenic trees in eight groups, and Rab4b is in a group also containing Rab2 (a and b), Rab4a, Rab11 (a and b) and Rab14 (Pereira-Leal and Seabra, 2001), which widely overlaps with a route of membrane traffic corresponding to recycling from endosomes to the cell surface (Stenmark, 2012). Large-scale profiling of Rab trafficking networks strongly suggests that Rab4b and Rab4a can fulfil different biological functions (Gurkan et al., 2005). This could be mainly due to differences in their respective enrichment, alongside that of their multiple partners in each cell type.

Of the Rab4 GTPases, Rab4a has been the most extensively studied, probably because it was discovered first. Its role is, however, not completely understood (reviewed by Grant and Donaldson, 2009), although it seems clear that it is associated with the early/recycling endocytic system (Sönnichsen et al., 2000). The early/recycling endocytic system is used by numerous molecules, including the transferrin receptors (TfRs), the prototype receptor for this pathway (Maxfield and McGraw, 2004). TfR enters cells by clathrin-dependent endocytosis. It is then delivered to early endosomes from which it can be sorted to the plasma membrane (fast recycling) or to the recycling endosomes. Recycling endosomes have a heterogeneous tubular-vesicular morphology and are defined by their accessibility for extracellular Tf and enrichment in markers such as Rab11 or Vamp3, and by the loss of early endosomal markers (EEA1, Rab5). TfR is also recycled from recycling endosomes back to the plasma membrane and this is referred to as the slow recycling pathway (Grant and Donaldson, 2009; Maxfield and McGraw, 2004). Overexpression of Rab4a favours Tf recycling from early endosomes, leading to an increased amount of TfR at the plasma membrane (McCaffrey et al., 2001; van der Sluijs et al., 1992). By contrast, the overexpression of inactive forms of Rab4a (Cormont et al., 2003; McCaffrey et al., 2001) and the overexpression of TBC1D16, a Rab4a GAP

(Goueli et al., 2012), inhibits TfR recycling. However, shRNA-mediated knockdown of Rab4a increases TfR fast recycling (Deneka et al., 2003). Numerous Rab4a effectors have been identified already. The overexpression of some of them, such as Rabip4 or D-AKAP2 induces a mixing of early and recycling endosomes, and decreases endosomal recycling and an inhibition of Tf recycling (Cormont et al., 2001; Eggers et al., 2009). The neuronal-specific Rab4a effector GRASP-1 also connects early and recycling endosomes (Hoogenraad et al., 2010). By contrast, overexpression of NDRG1 increases Tf recycling, whereas its downregulation inhibits Tf recycling (Kachhap et al., 2007). It is thus difficult to conclude on the exact role of Rab4a in endosomal trafficking, especially as all the studies were not performed on the same cells and also because the specificity of the Rab4a effectors for Rab4b has not been tested.

Only a small number of studies on Rab4b have been reported until now, and the trafficking step it controls has not been identified. In B lymphocytes, Rab4b expression is controlled in parallel with that of the major histocompatibility complex (MHC) class II, suggesting an important role in MHC-mediated antigen presentation (Krawczyk et al., 2007). Rab4b is a synapse-related gene that is affected in major depressive disorders in which synapses are lost in the dorsolateral prefrontal cortex (Kang et al., 2012). It could thus contribute to normal synapse genesis or function in this brain region. We found that, in adipocytes, Rab4b was partially colocalised with TfR (Kaddai et al., 2009), thus indicating that Rab4b is also an endocytic Rab. Its colocalisation with the Glut4 glucose transporters is greater than with TfR and the consequences of the downregulation of Rab4b in adipocytes strongly suggest its involvement in the control of Glut4 recycling between endosomes and their sequestration compartments (Kaddai et al., 2009): a role recently confirmed by Chen and co-workers (Chen et al., 2012). Because Rab4b is not only expressed in adipocytes, we set out to determine which endocytic trafficking steps it controls by studying TfR endocytic trafficking in HeLa cells expressing different levels of Rab4b.

Here, we establish a role for Rab4b in TfR trafficking between early and recycling endosomes in HeLa cells. Furthermore, we demonstrate that Rab4b interacts with the gamma subunit of the clathrin adaptor complex AP-1 (AP1γ). AP-1 is a heterotetrameric complex composed of two ~100 kDa subunits (γ and β1), a ~47 kDa subunit (μ1), and a ~20 kDa subunit (σ1). Two subunits, μ1A and μ1B exist and form the AP-1A and AP-1B adaptor complexes, respectively; the latter being exclusively expressed in epithelial cells. The hinge regions of γ- and β1-subunits bind clathrin and the appendage of the γ-subunit binds several accessory proteins. The μ1-subunits interact with tyrosine-based sorting motifs present on cargoes, and either they or the β1 subunit bind the dileucine-base motif (Bonifacino and Traub, 2003). We also found that Rab4b and AP1γ colocalise on clathrin-coated vesicles and TfR recycling is perturbed when Rab4b–AP1γ interaction is experimentally affected. Taken together, our results indicate that Rab4b and AP1γ cooperate for TfR trafficking.

Results

Rab4b controls the recycling of TfRs

To determine whether Rab4b participates in TfR recycling, we looked at the localisation of the two proteins. We used a cell line that expresses the murine form of Rab4b as a C-terminal fusion with GFP because no specific antibodies for Rab4b were available for immunofluorescence experiments. The overexpression of GFP-Rab4b was modest with a two- to threefold enrichment compared with the endogenous protein (supplementary material Fig. S1A). GFP-Rab4b and TfR were mostly colocalised in a perinuclear region and in peripheral structures (Fig. 1A). Colocalisation was detected in each confocal section. The 3D reconstructions of the GFP-Rab4b and TfR labelling were mostly superimposable (Fig. 1B). Immunogold labelling in electron microscopy indicated that GFP-Rab4b and TfR can be found on a continuous membrane in the same tubulo-vesicular structures that were in the close vicinity of a vacuolar early endosomes (Fig. 1C). GFP-Rab4b colocalised with Myc-Rab4a in a perinuclear region, but not in the periphery of the cell (Fig. 1D). A partial colocalisation between endogenous Rabip4 (Cormont et al., 2001), a Rab4a effector, as well as expressed DsRed-Rabip4 (supplementary material Fig. S1B,C) was also observed in a perinuclear region. The high degree of colocalisation between Rab4b and TfR suggests that it could be involved in TfR recycling. Its restricted colocalisation with Rab4a and its effector Rabip4 suggests that Rab4b could have a role that is different from Rab4a in TfR recycling.

Thus, we quantified the steady-state distribution of TfR in cells with modified levels of Rab4b expression (overexpressed and downregulated). To this aim, we used wild-type HeLa cells (wt) and HeLa cells stably expressing the murine form of Rab4b fused with N-terminal HA-tag (Ha-Rab4b). The two cell lines were further transfected with a siRNA directed against human Rab4b. The siRNA efficiently downregulated the expression of endogenous Rab4b mRNA without affecting the expression of Rab4a mRNA. It downregulated the expression of endogenous Rab4b, but not the expression of the exogenous murine HA-Rab4b (Fig. 2A). In addition, the expression of TfR was identical in the two cell lines treated or not with siRNA to knock down Rab4b (Fig. 2B). Its amount at the cell surface was, however, modified by changes in Rab4b expression. Indeed, Rab4b silencing in wt HeLa cells increased cell surface levels of the TfR, as attested by an increase in Tf binding at the plasma membrane. Conversely, Rab4b overexpression decreased cell surface levels of the TfR. Importantly, siRNA against Rab4b had no significant effect in cells expressing Ha-Rab4b (Fig. 2C), confirming that the observed effect was due to silencing of Rab4b. Similar results were obtained when HeLa cells expressing murine GFP-Rab4b were used (data not shown). In accordance with this change in steady state distribution of TfR, the distribution of TfR-containing vesicles on a glycerol gradient was affected by either an increased or decreased expression of Rab4b (supplementary material Fig. S2).

The increase in cell surface TfRs could result either from an inhibition of their internalisation or an increase in recycling. We thus measured the amount of internalised Tf in the same experimental conditions as before. HeLa cells (wt or expressing HA-Rab4b treated or not with anti-Rab4b siRNA) were incubated for increasing periods of time with labelled Tf and the intracellular amount was quantified at the end of the incubation. We observed that Tf uptake was proportional to the amount of cell surface TfR in each experimental condition, strongly suggesting that internalisation was not affected (Fig. 2D). This was confirmed by measuring the initial rate of internalisation (Fig. 2E). Labelled Tf was first incubated at 4℃ to allow its binding on cell surface TfRs. Its internalisation was then triggered by shifting the cells to 37℃. During the first minute, the

amount of intracellular Tf reached the same levels in cells expressing or not Rab4b, indicating that Rab4b does not play a role in Tf internalisation process. After 10 minutes of chase, the intracellular amount of Tf was more efficiently decreased in cells depleted for Rab4b than in control cells (Fig. 2E). In the absence of Rab4b, Tf is thus rapidly targeted back to the plasma membrane. This suggests that recycling could occur from early compartments of the endocytic process. We next measured the recycling from early endosomes by imaging-based techniques to quantify internalised fluorescent Tf. Fluorescent Tf was incubated at 20°C, a temperature that blocks Tf trafficking at the level of early endosomes (Mallard et al., 1998) and recycling was initiated by shifting the cells to 37°C. We observed that Tf recycling was slower in HeLa cells expressing GFP-Rab4b compared with the wt, whereas it was accelerated by Rab4b silencing in wt HeLa cells (supplementary material Fig. S3).

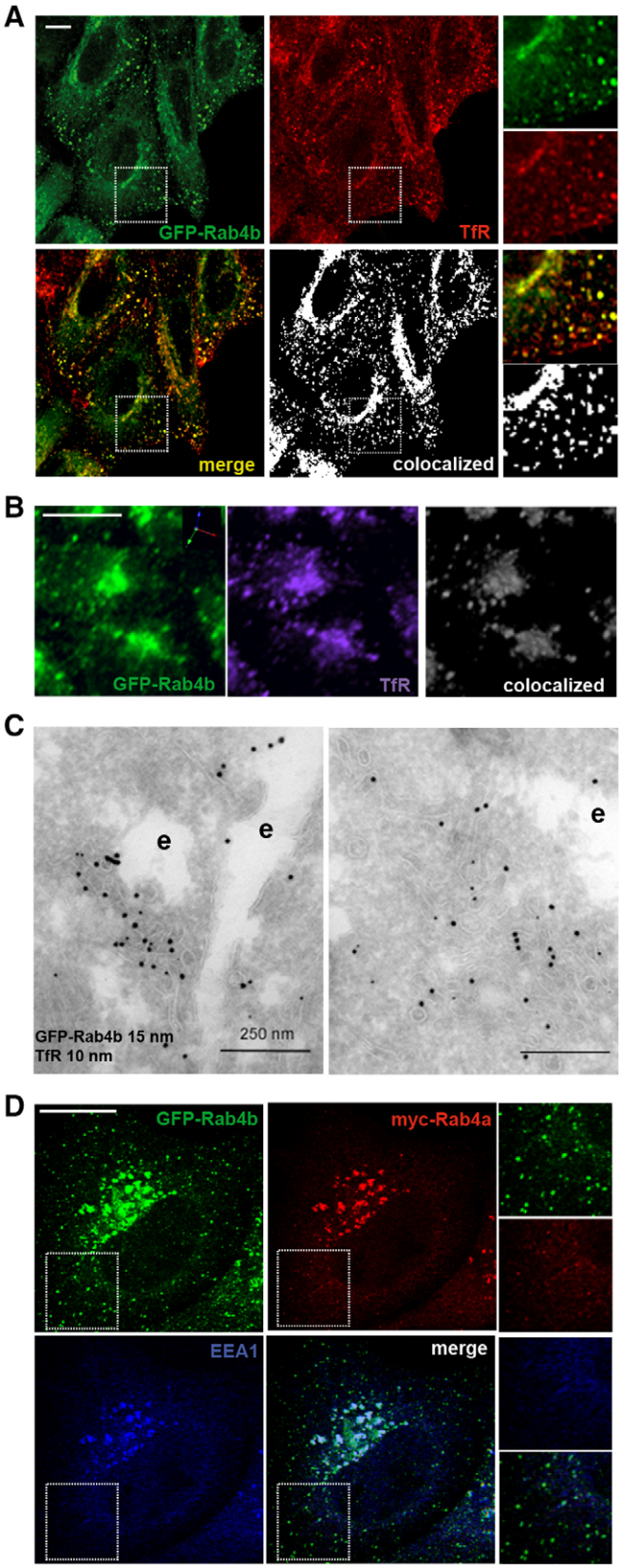

Rab4b is involved in an early endosome sorting event required for Tf to reach recycling endosomes

Tf is thought to recycle to the plasma membrane through a fast (from early endosomes) and a slow (from recycling endosomes) recycling pathway (for reviews, see Grant and Donaldson, 2009; Maxfield and McGraw, 2004). Thus, our results strongly suggest that Rab4b is involved in the control of the balance between these two pathways. We hypothesised that Rab4b could play a role in TfR sorting between early and recycling endosomes. Indeed, extracellular Tf reached GFP-Rab4b compartments and some of the GFP-Rab4b-containing structures were decorated with the early endocytic marker EEA1 (supplementary material Fig. S4A, arrows) whereas others, mostly located in the cell periphery, were not (supplementary material Fig. S4A, arrowheads). Extracellular Tf pre-bound to its receptor at 4°C first reached EEA1-positive vesicles and thereafter the GFP-Rab4b compartments when the temperature was shifted to 37°C (supplementary material Fig. S4B). We next tested whether extracellular Tf could reach recycling endosomes in the absence of Rab4b. To this aim, HeLa cells were transfected with Myc-Rab11 to label the recycling endosomes together with control or anti-Rab4b siRNA, and cells were incubated for 90 minutes with fluorescent Tf allowing it to equilibrate within its intracellular compartments (Fig. 3A). In control conditions, and as expected, extracellular Tf was detected in early endosomes (labelled with anti-EEA1 antibodies) and in recycling endosomes (labelled with exogenous Rab11). The most intense peaks of internalised Tf were colocalised with Myc-Rab11. In the absence of Rab4b, the most intense peaks of internalised Tf were found either with EEA1, or without both

Fig. 1. TfR and expressed Rab4b are colocalised in HeLa cells. HeLa cells expressing GFP-Rab4b were treated for TfR immunofluorescence. (A) Images of one confocal section corresponding to GFP-Rab4b (green), TfR (red), the merged image (merge) and the colocalised pixels (colocalised) are shown as well as enlarged views of the boxed regions. (B) A 3D reconstruction of GFP-Rab4b and TfR and the colocalised voxels obtained using Volocity software. (C) HeLa cells expressing GFP-Rab4b were treated for immunogold labelling in electron microscopy. GFP-Rab4b is detected with anti-GFP antibody followed by antibody against rabbit IgG coupled to 15 nm gold particles. Endogenous TfR is detected with anti-TfR antibody followed by antibody against mouse IgG coupled to 10 nm gold particles. e, endosomes. (D) HeLa cells expressing GFP-Rab4b were transiently transfected with pcDNA3-Myc-Rab4a and treated for immunofluorescence with anti-EEA1 antibodies. Images of one confocal section corresponding to GFP-Rab4b (green), Myc-Rab4a (red), EEA1 (blue), and the merged image (merge) are shown as well as enlarged views of the boxed regions. Scale bars: 10 μm (A,B,D); 250 nm (C).

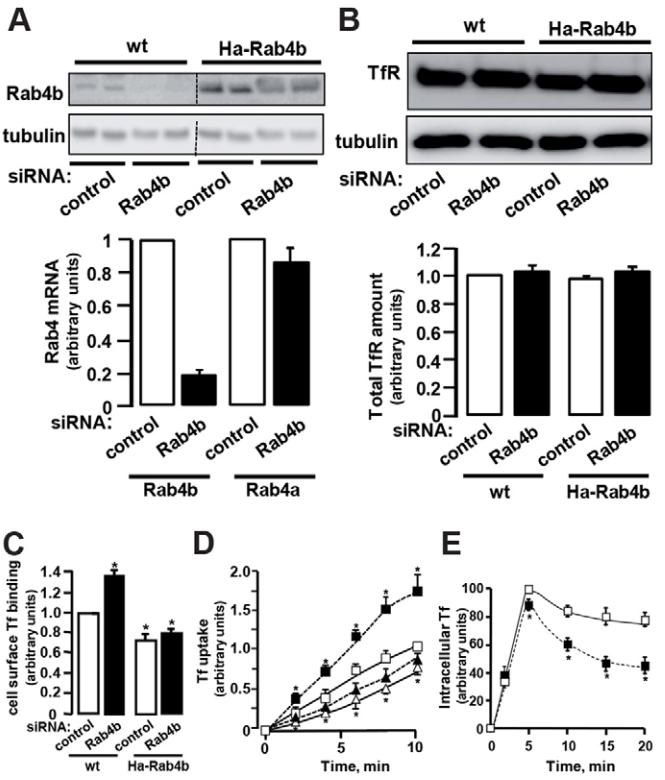

Fig. 2. Rab4b controls the recycling of TfR. Wild-type (wt) or Ha-Rab4b-expressing HeLa cells were transiently transfected with 10 nM of control or anti-Rab4b siRNA and the cells were used 48 hours later. (A) The amount of Rab4b was determined with an antibody against Rab4b (Kaddai et al., 2009) by western blotting. Tubulin was used as a loading control. The amount of mRNA encoding Rab4a and Rab4b was quantified by real-time PCR using RLP0 as an internal control. The graph represents the quantification ± s.e.m. of three independent experiments. (B) The amount of TfR was determined using a specific antibody. The expression of Rab4a was determined using a monoclonal antibody raised against recombinant Rab4a. Tubulin was used as a loading control. The graph represents the quantification of TfR amount in three independent experiments. (C) The amount of plasma membrane TfR was determined by saturation binding of HRP-coupled TfR. The results are expressed as the percentage of binding relative to the control condition (siRNA in wt HeLa cells) and the graph represents the mean ± s.e.m. of four experiments. (D) The capacity of the cells to internalise Tf was determined. Cells were incubated for up to 10 minutes with HRP-coupled Tf at 37℃. After incubation, the cells were subjected to acidic washes before quantifying internalised HRP-coupled Tf. The graph represents the mean ± s.e.m. of three experiments. (E) Cells were incubated with Alexa-Fluor-488-coupled Tf for 1 hour at 4℃ before shifting the cells to 37℃. Cells were subjected to acidic washes before quantification of internalised fluorescent Tf. The results are expressed as the percentage of the maximum for internalised Tf and are normalised to the plasma membrane amount of TfR determined in the same experiment. Open symbols are for cells treated with control siRNA whereas filled symbols correspond to cells treated with anti-Rab4b siRNA. Squares correspond to wt HeLa cells and triangles to HeLa cells overexpressing HA-Rab4b. *$P<0.05$ compared with control condition in wt cells.

EEA1 and myc-Rab11. Indeed, numerous peripheral vesicles containing only Tf were visible. In wt HeLa cells that did not overexpress Myc-Rab11a, internalised fluorescent Tf was also found in the periphery of cells when Rab4b was downregulated, rather than in the perinuclear region (supplementary material Fig. S4C). Fig. 3A also reveals that Rab4b silencing induced a change in the distribution of the recycling endosomes. When Rab4b was downregulated, Myc-Rab11 was found restricted to a central region of the cell, the labelled compartment had a more tubular appearance and fewer peripheral Rab11-containing vesicles were detected. It thus suggests that Rab4b is also important for the spatial organisation of Rab11-positive recycling endosomes.

Because Rab4b seemed to be required to target extracellular Tf to Rab11-positive recycling endosomes, we next determined whether overexpression of Rab4b could promote the entry of extracellular Tf into recycling endosomes. We previously observed that GFP-Rab4b and TfR were colocalised, and that internalised Tf was found mainly in GFP-Rab4b- and EEA1-positive perinuclear compartments, but also in more peripheral structures positive for Rab4b and negative for EEA1 (Fig. 3B). We thus questioned whether these latter structures contained markers of recycling endosomes. We first observed that mCherry-Rab11a was not enriched in these structures, whereas GFP-Rab4b and mCherry-Rab11a were partially colocalised in the perinuclear region (supplementary material Fig. S5). To avoid any bias linked to Rab11 overexpression, we determined whether these peripheral structures contained endogenous Vamp3, another marker of recycling endosomes (Daro et al., 1996). Vamp3 was also not detected in these GFP-Rab4b-positive structures in which Tf accumulated (Fig. 3B). The compartments labelled with anti-Vamp3 antibodies are likely to be recycling endosomes because Vamp3 partially colocalised with TfR but not with EEA1 in WT HeLa cells (supplementary material Fig. S6). Furthermore it was efficiently reached by internalised Tf in cells that did not express GFP-Rab4b (data not shown).

Taken together, these results indicate that Rab4b was required for Tf trafficking from early to recycling endosomes either because it directly controlled a trafficking event or because it perturbed the organisation of the recycling endosomes. Rab4b overexpression led to the genesis of structures that contained expressed Rab4b and were accessible to extracellular Tf, but devoid of early (EEA1) and recycling endocytic (Rab11/Vamp3) markers. This could suggest that intermediate vesicles of transport en route to recycling endosomes could somehow be accumulated when Rab4b was overexpressed.

Rab4b interacts with AP1γ and localises to clathrin-coated vesicles

To understand how Rab4b controls Tf trafficking between early and recycling endosomes, we searched for Rab4b effectors. By performing a screen with an active form of Rab4b (Rab4bQ67L) of a human placenta cDNA library in the yeast two-hybrid system we identified the γ-subunit of the clathrin adaptor complex 1 (AP1γ) as a putative Rab4b effector. We isolated a clone encoding a large region of the protein from amino acids 52 to 638. We next demonstrated that active Rab4bQ67L, but not inactive Rab4bS22N, interacted with the entire AP1γ subunit (1–822), and also with Rabip4 but not CD2AP, two previously described Rab4a effectors (Cormont et al., 2001; Cormont et al., 2003). Rab4bQ67L did not interact with the AP1γ-related adaptins from the AP-2 and AP-3 clathrin adaptor complexes, AP2α and AP3δ, respectively (Fig. 4A; supplementary material Fig. S7A). The other active mutants of endocytic Rab proteins, including Rab5, Rab6, Rab7 and Rab11, did not interact with either AP1γ or AP1γ (52–638) (Fig. 4B). We next determined which region of AP1γ was required to interact with Rab4b. Adaptins and AP1γ are organised in three distinct functional domains including the head

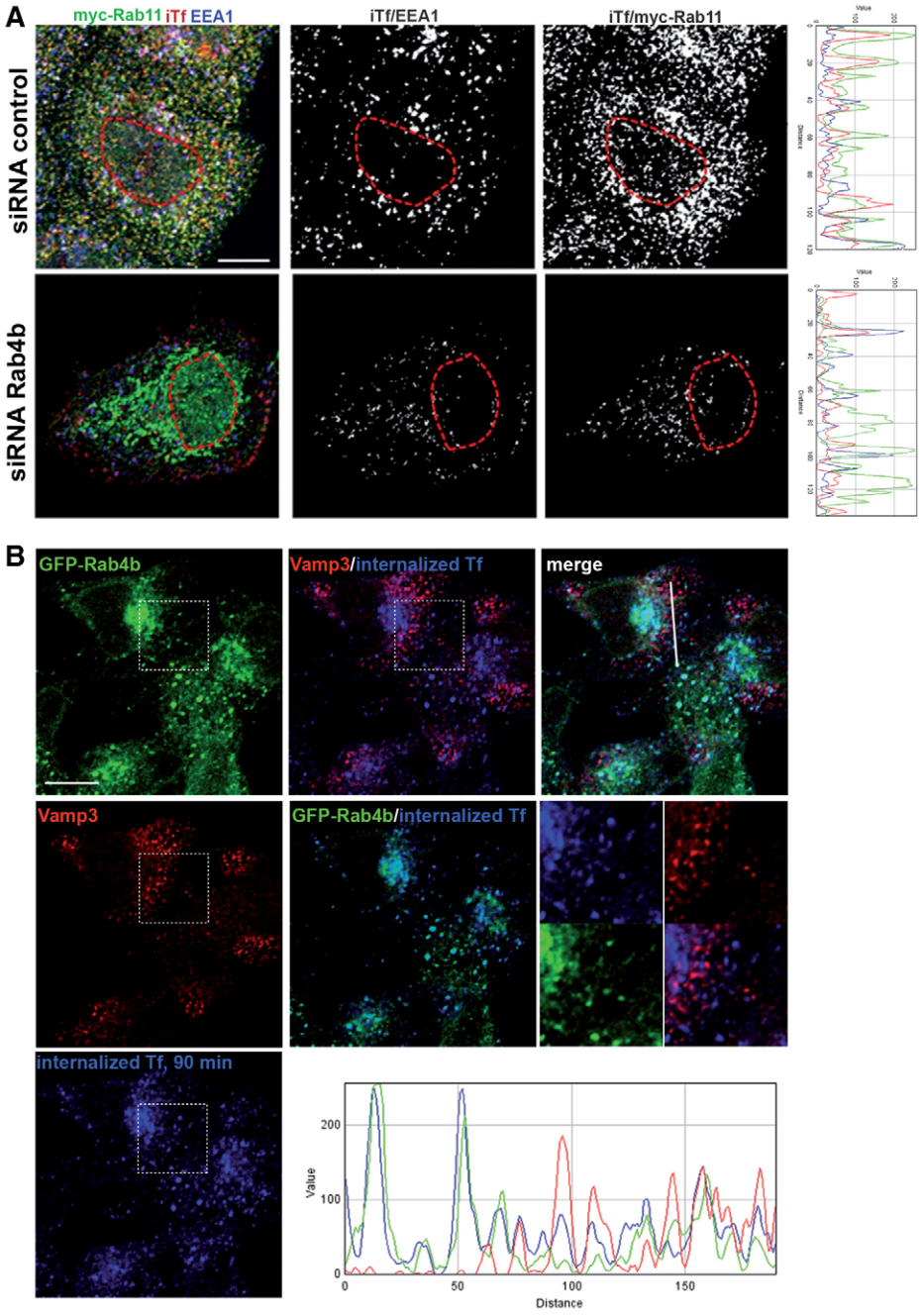

Fig. 3. Consequences of changes in Rab4b expression on Tf trafficking. (A) Wt HeLa cells were transfected with control or anti-Rab4b siRNA. After 24 hours, they were transfected with pCDNA3-Myc-Rab11 and cells were analysed 24 hours later for the capacity of extracellular Tf to reach Myc-Rab11-positive recycling endosomes in 90 minutes. The figure shows merged images of internalised Tf, Myc-Rab11 and EEA1 and the colocalised pixels between internalised Tf and either EEA1 or Myc-Rab11. A dotted line delineates the nucleus, which is slightly labelled by anti-Myc antibodies. The right panels show the intensity profile along a line for each label. (B) HeLa cells stably expressing GFP-Rab4b were incubated with Alexa-Fluor-680-coupled Tf for 90 minutes. Endogenous Vamp3 was then detected by indirect immunofluorescence. The figure shows the confocal images obtained for GFP-Rab4b, Vamp3 and internalised Tf and merged images (merge) as indicated. Enlarged views of the delineated regions and a profile analysis made along a line with ImageJ are shown. Scale bars: 10 μm.

and trunk N-terminal domain (1–595), the hinge (595–703) and the ear domains (703–822). We observed that the interaction was lost when the first 488 amino acids were deleted. Because AP1γ (479–638) interacted with Rab4b, we concluded that the interaction occurred between amino acids 479 and 638, located between the head and the hinge domain of AP1γ (Fig. 4C). We named this domain AP1γ-RBR for AP1γ Rab4b-binding region.

We confirmed an interaction between AP1γ and Rab4b in co-immunoprecipitation experiments. Overexpressed HA-Rab4b co-immunoprecipitated with endogenous AP1γ when anti-AP1γ antibodies were used compared with a non-relevant one (control mouse IgG, NR). Furthermore, a non-relevant endocytic HA-tagged protein, HA-CIN85, was not co-immunoprecipitated with AP1γ (Fig. 4D). We also detected co-immunoprecipitation between endogenous AP1γ, but not AP2α or AP3δ, and overexpressed HA-Rab4b when HA-Rab4b was immunoprecipitated from transiently transfected HEK293 cells (mock-transfected cells were used as a control) (Fig. 4E; supplementary material Fig. S7). Similar results were obtained when HeLa cells stably expressing HA-Rab4b and wt HeLa cells were used to perform anti-HA co-immunoprecipitation (Fig. 4F). We also observed that recombinant His-tagged AP1γ interacted more efficiently with active GST-Rab4b (GTPγS-loaded) than with its inactive form (GDP) in a pull-down experiment (Fig. 4G).

AP1γ is one subunit of the hetero-tetrameric AP-1 complex that binds clathrin. As expected, the β-subunit of the clathrin adaptor complex AP-1 as well as clathrin heavy chain (CHC)

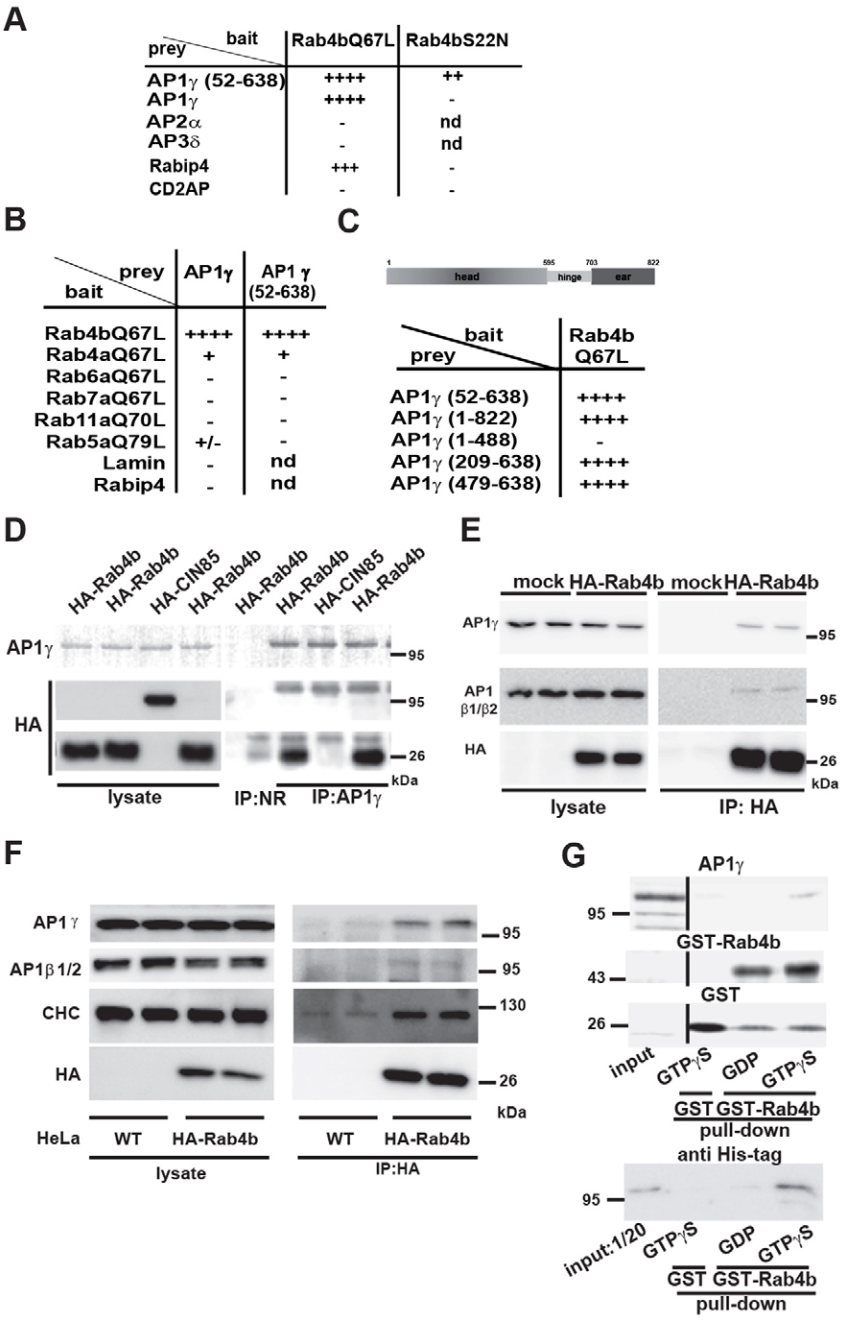

Fig. 4. Characterisation of the interaction between AP1γ and Rab4b. (A,B,C) L40 reporter yeasts were co-transformed with vectors encoding the indicated baits and preys. Yeast was grown in the absence of Leu and Trp and β-galactosidase activity was determined on replicate filters using X-gal as a substrate. ++++, blue colouration appeared within 30 minutes; ++, colouration appeared after 2 hours; +, colouration appeared in 6 hours; +/−, colouration appeared after 24 hours; −, no colouration was obtained after 24 hours. The expression of all constructs was checked by western blotting on yeast lysates (data not shown). (D) HEK293 cells were transiently transfected with HA-Rab4b or HA-CIN85. 36 hours later, lysates were prepared and subjected to immunoprecipitation using anti-AP1γ or non-relevant antibodies (NR). Total lysates and proteins associated with the pellet were subjected to SDS-PAGE and transferred to PVDF membrane. The blot was incubated with anti-AP1γ or anti-HA antibodies and revealed using TrueBlot HRP-coupled anti-mouse antibodies (eBioscience) and ECL reagent. Capture of the images was made with a Fuji LAS 3000. (E) HEK293 cells were transiently transfected with pcDNA3-HA-Rab4b or the corresponding empty vector (mock). Lysates were subjected to immunoprecipitation with anti-HA antibodies. The immune pellets were analysed for the presence of AP1γ, AP1β1/β2 or HA as described above. (F) HeLa cells, wt or stably expressing HA-Rab4b, were subjected to immunoprecipitation with anti-HA antibodies. Total lysates and proteins associated with the pellet were analysed on a western blot to detect HA-Rab4b, AP1γ, AP1β1/2 and CHC. (G) A pull-down experiment was performed using GST, GST-Rab4b loaded with GDP or GTPγS immobilised on glutathione-Sepharose in the presence of recombinant His-tagged AP1γ.

was found associated with Rab4b in co-immunoprecipitation experiments (Fig. 4E,F). This suggests that Rab4b can interact with the entire AP-1 complex, leading to clathrin recruitment. In accordance with an interaction between Rab4b and AP1γ, we also observed that GFP-Rab4b and AP1γ, but not AP2α, were colocalised in HeLa cells, both in the perinuclear region and in punctuated peripheral structures (Fig. 5A; supplementary material Fig. S7C). Small amounts of AP3δ labelling were detected within the GFP-Rab4b structures in the periphery of the cells, but the majority of the AP3δ-containing vesicles did not contain GFP-Rab4b (supplementary material Fig. S7D). Furthermore, the expression of GFP-Rab4b perturbed AP1γ labelling, which was mostly concentrated in the Golgi area in wt HeLa cells (not shown). Most of these structures also contained internalised Tf, and expressed Rab4b was also partly colocalised with endogenous CHC (supplementary material Fig. S8A,B) and clathrin light chain (GFP-LCa, supplementary material Fig. S8C). Rab4b and CHC colocalised in perinuclear EEA1-positive structures and in peripheral EEA1-negative structures (supplementary material Fig. S8B). Immuno-EM allowed us to highlight tubules and vesicles decorated by antibodies against GFP-Rab4b and endogenous AP1γ that were located in tubulo-vesicular regions close to an endosome. Structures positive for GFP-Rab4b and GFP-AP1γ were coated in a manner resembling clathrin-coated vesicles (Fig. 5B). They did not present similarities with the flat bilayered clathrin lattice used by ubiquitylated cargoes to enter late multi-vesicular endosomes (Raiborg et al., 2002; Sachse et al., 2002). They looked rather like clathrin-coated

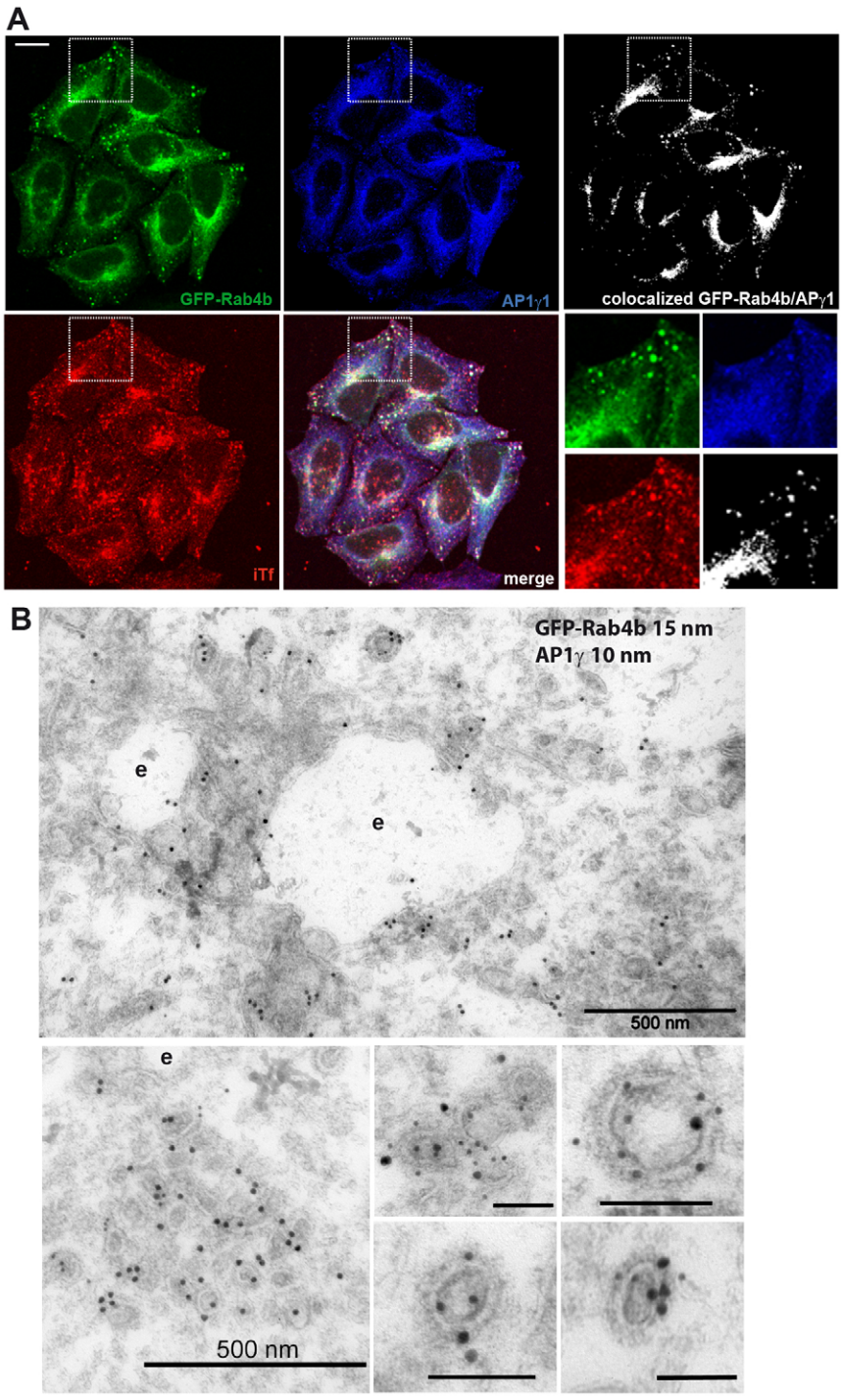

Fig. 5. AP1γ colocalises with GFP-Rab4b. (A) HeLa cells expressing GFP-Rab4b were incubated for 90 minutes with Texas-Red-coupled Tf. They were then treated for indirect immunofluorescence with anti-AP1γ antibodies. Cells were analysed by confocal microscopy. The figure shows the labelling corresponding to GFP-Rab4b (green), AP1γ (blue), internalised Tf (iTf, red) and the colocalised points between GFP-Rab4b and AP1γ. The boxed regions are also shown enlarged. Scale bar: 10 μm (B) HeLa cells stably expressing GFP-Rab4b were treated for immunodetection in electron microscopy. Antibodies against GFP were used to detect GFP-Rab4b followed by secondary antibodies coupled to 15 nm gold particles. AP1γ is detected with anti-AP1γ antibody and secondary antibodies coupled to 10 nm gold particles. The figure shows typical labelling in tubulo-vesicular regions near early endosomes (e) and enlarged views (scale bars: 100 nm) of coated structures containing both AP1γ and GFP-Rab4b found in these tubulo-vesicular regions.

tubulo-vesicular structures emanating from vacuolar early endosomes. Taken together, the co-immunoprecipitation of Rab4b with CHC and their colocalisation in electron and immunofluorescent microscopy strengthen the idea that Rab4b could organise the clathrin coat on Rab4b-positive endosomes.

Interaction between AP1γ and Rab4b is required for control of TfR recycling

Our results suggested that Rab4b could be involved in the recruitment of a clathrin coat involved in the formation of vesicles en route to recycling endosomes through its interaction with AP1γ. The increase or decrease in Rab4b expression did not change the distribution of AP1γ between the cytosol and the membranes (data not shown). However, silencing of Rab4b induced a loss of AP1γ in light density membrane fractions separated on a glycerol gradient (supplementary material Fig. S9). Rab4b could thus be required for the association of AP1γ with a subtype of intracellular vesicles. Interestingly, in HeLa cells expressing similar levels of GFP-Rab4a and GFP-Rab4b (GFP-Rab4a cln1), we did not detected numerous peripheral

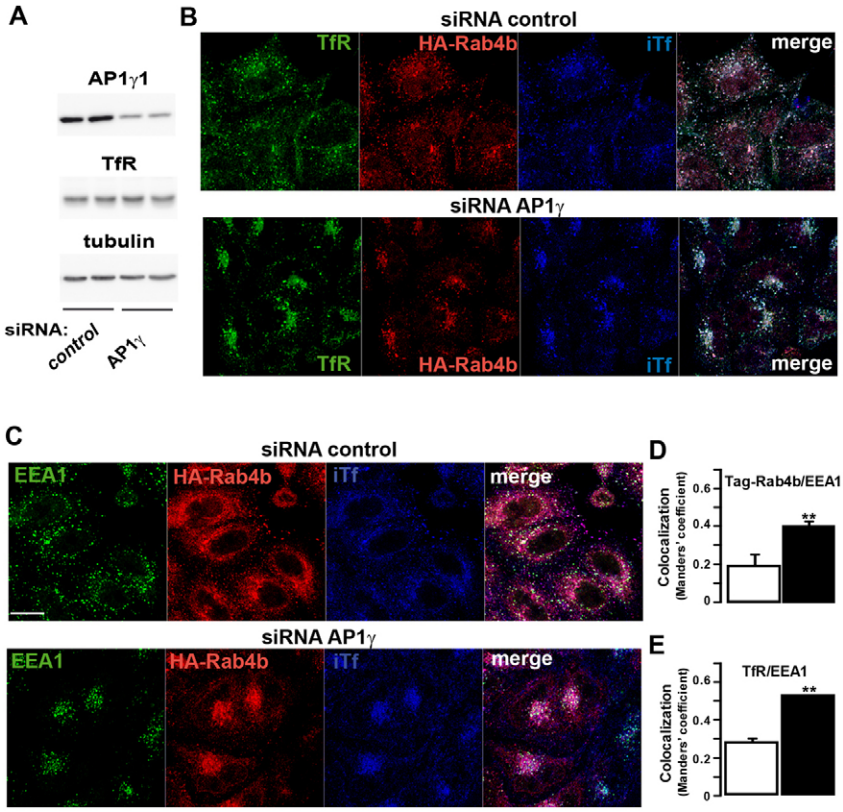

Fig. 6. AP1γ is required for the formation of Rab4b-positive, EEA1-negative TfR-containing vesicles. HeLa cells expressing HA-Rab4b were transfected with control or anti-AP1γ siRNA and used 48 hours later. (A) Lysates were prepared to determine the amount of AP1γ and TfR by western blotting. Tubulin was used as loading control. (B) Cells were incubated for 90 minutes with Alexa-Fluor-680-coupled Tf before treatment for immunofluorescence of TfR and HA tag. Cells were analysed by confocal microscopy and images corresponding to TfR (green), HA-Rab4b (red), internalised Tf (iTf, blue) and the merged image of the three labels are shown. (C) Cells were incubated for 90 minutes with Alexa-Fluor-680-coupled Tf before treatments for immunofluorescence of EEA1 and the HA tag. Cells were analysed by confocal microscopy for EEA1 (green), HA-Rab4b (red) and internalised Tf (iTf, blue); merged images of the three labels are shown. (D) Confocal images of the experiment shown in C analysed using the JaCOP plug-in of ImageJ software to determine the extent of colocalisation of tagged-Rab4b with the EEA1-positive structures. White column shows control siRNA whereas the black one shows anti-AP1γ siRNA. (E) The extent of colocalisation between TfR and EEA1 was determined as above in wild-type HeLa cells treated with control (white column) or anti-AP1γ siRNA (black column). For D and E, four images were taken for each condition and the experiment was repeated three times. The graph shows the mean ± s.e.m. of the Manders' coefficient corresponding to tagged-Rab4b or TfR channel within the EEA1 channel. Differences are significant with $*P<0.05$ and $**P<0.005$ (unpaired Student's *t*-test). Scale bars: 10 μm.

structures containing both GFP-Rab4a and AP1γ, whereas such peripheral structures were detected when GFP-Rab4a was overexpressed to a higher level than GFP-Rab4b (supplementary material Fig. S10A–E). We next determined whether AP1γ was involved in the control of Rab4b-containing compartments. We thus aimed to silence AP1γ in HeLa cells stably expressing HA-Rab4b. The use of siRNA against AP1γ yielded up to 60% inhibition of the protein expression compared with the control, and did not affect TfR expression (Fig. 6A). The inhibition occurred with a similar efficiency in each cell as proved by indirect immunofluorescence with anti-AP1γ antibody (data not shown). We observed that the compartments containing HA-Rab4b and TfR were more concentrated in the centre of the cells when the expression of AP1γ was decreased. Internalised Tf was also accumulated in these compartments. This suggested that the peripheral Rab4b-positive, EEA1-negative vesicles could not be formed in the absence of AP1γ (Fig. 6B). In accordance, the extent of colocalisation between HA-Rab4b and EEA1 was increased in cells with lower expression of AP1γ (Fig. 6C,D). Indeed, there were nearly no structures labelled with HA-Rab4b that were accessible to internalised Tf except for the EEA1-positive structures. Furthermore, the extent of colocalisation between TfR and EEA1 was also increased in wt HeLa cells expressing lower amounts of AP1γ (Fig. 6E).

Rab4b could thus favour the sorting of TfR from early endosomes by interacting with AP1γ. We thus wanted to determine the consequence of a block of the interaction between Rab4b and AP1γ. We thus constructed a vector encoding a fusion protein consisting of N-terminal GFP, the Rab4b-binding region of AP1γ and a C-terminus of the two Fyve fingers from Hrs (GFP-AP1γ-RBR-Fyve), which are specifically targeted to PI3P-enriched early endosomes (Gaullier et al., 1998). We verified that overexpression of this protein inhibited the interaction between HA-Rab4b and AP1γ (Fig. 7A). HEK293 cells expressing HA-Rab4b and either GFP-Fyve or GFP-AP1γ-RBR-Fyve were subjected to immunoprecipitation with anti-HA antibodies. We clearly observed that the amount of AP1γ associated with HA-Rab4b was decreased by the expression of GFP-AP1γ-RBR-Fyve compared with GFP-Fyve. We next determined whether the recycling of internalised Tf was affected by the overexpression of GFP-AP1γ-RBR-Fyve. For this, wt HeLa cells overexpressing either GFP-Fyve or GFP-AP1γ-RBR-Fyve were incubated for 5 minutes with Texas-Red-coupled Tf at 37℃, washed, and reincubated with non-labelled holo-Tf to prevent reinternalisation of fluorescent Tf. Fifteen minutes later, cells were processed for confocal imaging. The remaining amount of intracellular Tf in GFP-AP1γ-RBR-Fyve-expressing cells was increased compared with the surrounding non-transfected cells. This was not observed when the cells overexpressed GFP-Fyve (Fig. 7B,C). The amount of fluorescent Tf internalised during the first 5 minutes of incubation was, however, similar in cells either expressing or not the different GFP-fusion proteins (not shown). These observation indicated that the overexpression of GFP-AP1γ-RBR-Fyve inhibited the recycling of Tf. Intracellular Tf was blocked in compartments labelled with GFP-AP1γ-RBR-Fyve (Fig. 7B) that were also positive for EEA1 (not shown), thus indicating that the block occurred in early endosomes. These results also strongly suggested that the interaction between Rab4b and AP1γ is required for early endocytic sorting of TfR. But in these

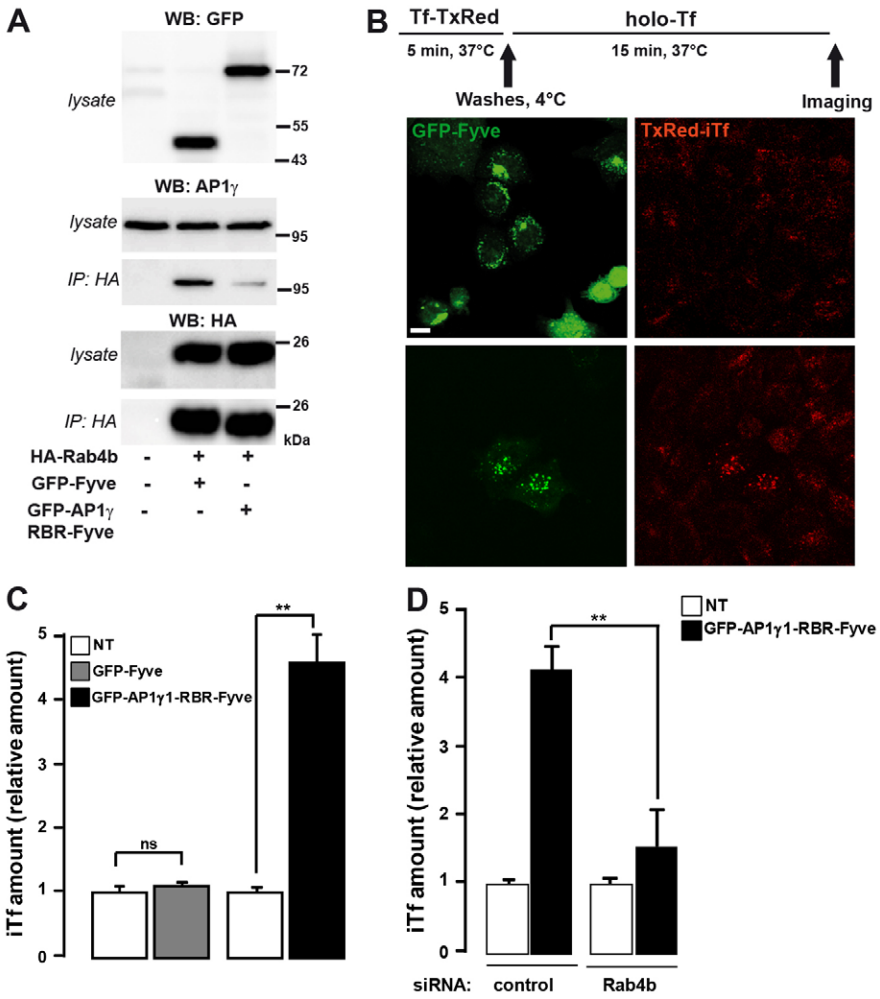

Fig. 7. Expression of GFP-AP1γ-RBR-Fyve inhibits the recycling of internalised Tf. (A) HEK293 cells were transfected with mock vector or HA-Rab4b, with either GFP-Fyve or GFP-AP1γ-RBR-Fyve. 24 hours later, lysates were submitted to immunoprecipitation using anti-HA antibodies. Total lysates and proteins associated with the pellets were subjected to western blotting with anti-AP1γ, anti-HA or anti-GFP antibodies, and revealed using TrueBlot HRP-coupled antibodies against mouse IgG for AP1γ and HA (eBioscience) or HRP-coupled antibodies against rabbit IgG for GFP. (B) Wt HeLa cells were transiently transfected with pEGFP-Fyve or pEGFP-AP1γ-RBR-Fyve. 24 hours later, cells were incubated for 5 minutes at 37℃ with Texas-Red-coupled Tf. After an acid wash and three washes in PBS at 4℃, cells were incubated with an excess of unlabelled holo-Tf for 15 minutes. Cells were then fixed and analysed by confocal microscopy. The figure shows representative fields with HeLa cells overexpressing or not the GFP-fusion proteins. Scale bar: 10 µm. (C) The amount of intracellular Tf (iTf) was quantified in cells expressing the GFP-fusion protein and in surrounding non-transfected cells (NT). 150 transfected and non-transfected cells were analysed in three independent experiments. In each analysed field, the amount of iTf for each cell was normalised to the amount of iTf in one of the non-transfected cells. ns, not significant; $^{**}P<0.0001$ (Mann–Whitney). (D) Wt HeLa cells were transfected with control or anti-Rab4b siRNA. 24 hours later they were transfected with pEGFP-AP1γ-RBR-Fyve. Tf recycling was studied as in B, and images were quantified as above. $^{**}P<0.005$.

experimental conditions and in contrast to what happens in the absence of Rab4b, Tf was not rapidly recycled back to the plasma membrane. The inhibition of Tf recycling induced by the overexpression of GFP-AP1γ-RBR-Fyve required Rab4b because it did not occur in its absence. The observed inhibition was thus probably due to a loss of interaction between Rab4b and endogenous AP1γ (Fig. 7D).

Discussion

TfR recycles between intracellular compartments and the plasma membrane either from early endosomes (fast recycling) or from recycling endosomes (slow recycling), implying that it also traffics from early to recycling endosomes (Grant and Donaldson, 2009). Numerous Rab proteins are involved in TfR recycling, but a potential role of Rab4b has not been investigated. Here, we show that Rab4b is required for intracellular trafficking of TfR. The Rab4b-dependent step could be the passage between early and recycling endosomes because inhibition of Rab4b expression increased TfR fast recycling, whereas Rab4b overexpression had the opposite effect. Furthermore, inhibition of Rab4b expression prevented Tf from efficiently reaching Rab11-positive endosomes.

Surprisingly, although Rab4b expression inhibited TfR fast recycling, it did not allow the efficient entry of Tf into recycling endosomes. Indeed, internalised Tf–TfRs that were no longer in EEA1-positive early endosomes were not localised in vesicles enriched for markers of recycling endosomes. These structures could be transport intermediaries between early and recycling endosomes and thus, some cargoes could be retained within the cell in a Rab4b-dependent manner. We previously observed that Rab4b was required for the basal retention of the glucose transporter Glut4 in adipocytes that express high level of Rab4b (Kaddai et al., 2009). It remains unclear why silencing of Rab4b did not affect the steady state distribution of TfR in adipocytes (Kaddai et al., 2009). We suggest this is due to a difference in technique sensitivity used to measure plasma membrane TfR. The Rab4b-dependent step could also be an active sorting step dependent on cargo-sorting signals. If a motif in Glut4, which is highly expressed in adipocytes, is more efficiently recognised by the sorting machinery than a motif on TfR, it could compete for TfR sorting.

We found that Rab4b was required for Tf delivery into Rab11- and Vamp3-positive recycling endosomes and that its overexpression induced the formation of Rab4b-positive, EEA1-negative structures that did not contain markers of recycling endosomes but rather of Tf–TfRs. This suggested that a vesicle budding/fusion mechanism exists for trafficking between early and recycling endosomes, and that it could be controlled by Rab4b. It has previously been proposed that trafficking between early and recycling endosomes occurs under a Rab conversion model (Sönnichsen et al., 2000) similar to the early-to-late

endocytic pathway (Poteryaev et al., 2010; Rink et al., 2005). Coordination between endocytic Rab proteins certainly exists because they share some of their effectors (Galvez et al., 2012) and this could explain why the morphology of the Rab11-positive compartment was widely affected by Rab4b silencing. Tubules and subsequent vesicles are formed as endosomes undergo Rab4a-to-Rab11 transition (van Weering et al., 2012), in accordance with a budding process at the early-to-recycling-endosome step. Furthermore, Sonnichsen and co-workers described GFP-Rab4a-containing vesicles without markers of early (Rab5) and recycling endosomes (Rab11) (Sönnichsen et al., 2000), similar to those we observed with GFP-Rab4b. However, they represent a minority of the Rab4a-containing endosomes, whereas we estimated that 50% of GFP-Rab4b-positive structures are neither in early (EEA1 negative) nor in recycling endosomes (Rab11 or Vamp3 negative), despite containing TfRs. A budding process is also supported by the *in vitro* budding assay from early endosomes of vesicles containing the recycling receptor asialoglycoprotein receptor H1 developed by Pagano and co-workers (Pagano et al., 2004). Even more interestingly, this *in vitro* budding required Rab4, but the tools used did not permit discrimination between Rab4a and Rab4b. Rab4 expression also induces the formation of synaptic-like microvesicles in an *in vitro* assay of early endosome budding (de Wit et al., 2001). Their comparison of HeLa cells expressing the same levels of GFP-Rab4b and GFP-Rab4a strongly suggests that Rab4b is more efficient at inducing the formation of GFP-Rab4-positive, EEA1-negative peripheral structures. In accordance, we found that GFP-Rab4b expression inhibited plasma membrane TfR localisation, whereas that Rab4a increased it when expressed at the same level, as previously described (McCaffrey et al., 2001; van der Sluijs et al., 1992).

The existence of a budding process controlled by Rab4b was reinforced because we found that Rab4b interacted with the AP1γ subunit of the clathrin adaptor complex, AP-1, known for its involvement in clathrin-dependent vesicle budding at the TGN (Robinson and Bonifacino, 2001). It remains to be determined whether the interaction between active Rab4b and AP1γ is direct, because indirect interactions could sometimes be detected in yeast two-hybrid screens and because the recombinant His-tagged AP1γ we produced was not pure. Indeed, a previous study suggested that an AP1γ–AP1σ subcomplex of AP-1 interacted with active Rab4a through Rabep1/2 (Deneka et al., 2003). The authors found that the ear domain of AP1γ interacted with Rabep1/2 and that active Rab4a was able to precipitate Rabep1/2 and AP1γ from pig brain cytosol. However, they did not prove that the interaction between Rab4a and AP1γ required Rabep1/2. Additional experiments will thus be required to understand the mechanisms involved in the recruitment of AP1γ by Rab4b and to determine the contribution of other proteins, including the other subunits of AP-1, in the formation and stability of the interaction. Also, we cannot exclude that other Rab proteins, among the many found in endosomes, could interact with AP1γ. AP-1 was also involved in retrograde transport of several cargoes from early endosomes to TGN, but the involvement of clathrin in this AP1-dependent pathway is still under discussion (Johannes and Popoff, 2008; Pfeffer, 2011). Budding of clathrin-coated vesicles from endosomes is described at the ultrastructural level, although they were found only occasionally associated with AP1γ (Stoorvogel et al., 1996). Also, budding of vesicles containing AP-1 and coated with clathrin was also found on common recycling endosomes (CREs) in epithelial cells (Futter et al., 1998). Interestingly, the Rab4-dependent *in vitro* budding process of recycling molecules from early endosomes was also dependent on AP-1 and clathrin (Pagano et al., 2004). Thus it suggested that recycling receptors could be sorted from early endosomes by an AP-1- and clathrin-dependent budding process. In accordance, we found that Rab4b associated with AP1γ and clathrin heavy chain in co-immunoprecipitation experiments. GFP-Rab4b, AP1γ, clathrin heavy and light chain also colocalised in immunofluorescence studies, and GFP-Rab4b- and AP-1γ-containing tubules and vesicles were found around early endosomes decorated in a manner reminiscent of clathrin coats. Changes in Rab4b expression modified the density of TfR-containing vesicles and Rab4b silencing induced AP1γ loss in light vesicles, thus suggesting that Rab4b could control coat formation on TfR-containing budding vesicles. Furthermore, the inhibition of AP1γ expression in Rab4b-expressing cells induced the loss of the more peripheral GFP-Rab4b-containing vesicles concomitantly with an increased colocalisation of GFP-Rab4b and TfR in early EEA1-positive endosomes. Interestingly, a similar change in TfR localisation was reported in cells overexpressing the dominant-negative clathrin inhibitor Hub (Bennett et al., 2001). Taken together, our results thus strongly suggest that Rab4b could coordinate the formation of TfR-containing clathrin-coated vesicles.

Previous reports described that AP-1 is involved in Tf recycling (Delevoye et al., 2009; Gravotta et al., 2012) and suggested that AP-1 interacts with TfRs (Gravotta et al., 2012). In epithelial cells, the basolateral sorting of TfR required AP-1A and AP-1B. AP-1A targets the TfR to the basolateral plasma membrane from the TGN, whereas AP-1B has been proposed to permit TfR recycling from CREs to the basolateral membrane (Gravotta et al., 2012). However, this could be a consequence of the mistargeting of TfRs to the apical plasma membrane, indeed suggesting that AP-1B is required to maintain TfRs within the basolateral recycling pathway. The different role of the two AP-1 complexes has been explained by their different localisation, AP-1A localising predominantly at the TGN, whereas AP-1B was enriched in the TfR-containing CREs. μ1B, but not μ1A, was indeed shown to interact with CRE-enriched phospholipid PIP3 (Fields et al., 2010). In melanocytes, AP-1 silencing by anti-μ1 or anti-γ siRNA accelerated Tf recycling from early endosomes to the plasma membrane (Delevoye et al., 2009). We also observed that AP1γ silencing increased the number of plasma membrane TfRs without affecting Tf internalisation (data not shown) in a manner similar to inhibition of Rab4b, supporting such a role in HeLa cells. Rab4b could thus recruit AP-1 to early endosomes in HeLa cells that did not express μ1B (Ohno et al., 1999), and it could thus play a role in the general endocytic recycling pathway. We think that Rab4b probably interacts more efficiently with AP1γ than Rab4a, because when Rab4b and Rab4a are overexpressed to the same extent, Rab4b but not Rab4a induces the formation of Rab4-positive, AP1γ-positive, EEA1-negative peripheral structures. However, Rab4a could interact with AP1γ as demonstrated in yeast two-hybrid screens and a higher level of Rab4a induced the formation of these structures (supplementary material Fig. S10C,E) and decreased the amount of TfR at the plasma membrane (supplementary material Fig. S10F).

Taken together, our results suggest that Rab4b and AP-1 are required to target TfRs outside the fast recycling pathway. In accordance, the inhibition of endogenous Rab4b and AP1γ

interaction through the use of endocytic expression of the domain of AP1γ that interacted with Rab4b (GFP-AP1γ-RBR-Fyve) blocked TfRs in early endosomes. Under these conditions, TfRs could be engaged in the trafficking pathway to the recycling endosomes but could not be directed either in the fast or in the slow recycling pathway. We do not know the molecular mechanisms involved. They are certainly linked to the fact that Rab4b remained in interaction with GFP-AP1γ-RBR-Fyve, but we could not rule out the possibility that overexpression of GFP-AP1γ-RBR-Fyve blocked the TfR in early endosomes by interacting with Rab4a.

In conclusion, we found that Rab4b is an important player in the control of the steady-state distribution of TfRs because it permitted their early endocytic sorting to recycling endosomes. At the molecular level, this sorting step required the interaction between Rab4b and AP1γ that allows for AP-1-dependent budding of TfR-containing vesicles coated with clathrin. Also of interest, our results suggest that Rab4b expression could permit generation of a novel type of endocytic vesicles that are low in early and recycling endocytic markers (schematised in supplementary material Fig. S10G). It is tempting to speculate that they could constitute specialised storage compartments in cells that naturally express high levels of Rab4b.

Materials and Methods

Antibodies

Antibodies against Vamp3 were a gift from Dr Thierry Galli (Institut Jacques Monod, Paris, France). Rabip4 antibodies were described previously (Mari et al., 2006). Rab4b antiserum was produced by immunising rabbits with the C-terminal peptide of Rab4b coupled to KLH (Eurogentec, Liège, Belgium). mAb 100/3 against AP1γ and tubulin were from Sigma-Aldrich (St Louis, MO). mAb 100/2 (Sigma-Aldrich) and mAb AP6 (Thermo Scientific, Rockford, IL) against α-adaptin was used in western blot experiments and immunofluorescence, respectively. mAb against EEA1, anti δ-adaptin and Rab4 and rabbit polyclonal anti-GFP antibodies were from BD Biosciences (Palo Alto, CA). Rabbit mAb anti-EEA1 was from Cell Signaling Technology (Danvers, MA). Rabbit polyclonal anti-GFP antibody for electron microscopy was from ICL (Portland, OR). mAb anti-HA was from Covance (Hemeryville, CA) and rabbit serum anti-HA was from MBL International (Clinisciences, Nanterre, France). mAb anti-TfR and Alexa-Fluor-488-coupled secondary antibodies were from Invitrogen (Camarillo, CA). mAb anti-APβ1/2 (100/1) was from Santa Cruz Biotechnology. mAb X22 anti-CHC was from Thermo Scientific (Rockford, IL). mAb anti-Myc was from Roche Diagnostics (Indianapolis, IN). HRP-, Texas-Red- and Cy5-coupled anti-species antibodies and Tf-HRP were from Jackson ImmunoResearch Europe (Newmarket, UK). 10-nm-Gold-coupled goat anti-mouse IgG and 15-nm-Gold-coupled goat anti-rabbit IgG for electron microscopy were from BBInternational (Cardiff, UK).

Plasmids

pEGFP-Rab4b and pcDNA3-HA-Rab4b were described previously (Kaddai et al., 2009). pEGFP-Rab4a, Myc-Rab4a, pDsRed-Rabip4, pcDNA3-Myc Rab11b, pLex-Rab4aQ67L/S22N, pLex-lamin, pLex-Rabip4, pAct-Rabip4, pAct-CD2AP have also been described (Cormont et al., 2001; Cormont et al., 2003). pEGFP-Fyve was a gift from Dr H. Stenmark (Centre for Cancer Biomedicine, Montebello, Norway). pLex-Rab5aQ79L, Plex-Rab6aQ72L and pIRES-Hygro-mCherry-Rab11a were gifts from Dr Bruno Goud (Institut Curie, Paris, France). pLex-Rab7aQ79L was a gift from Dr Cecilia Bucci (Salento University, Lecce, Italy). pLex-Rab11aQ70L was a gift of Dr Jean Salamero (Institut Curie, Paris, France). pACT2-AP1γ was provided by Dr J. Bonifacino. pACT2-AP2α and pGAD-AP3δ were provided by Dr A. Benmerah. pEGFP-LCa was a gift from Dr P. Cossart (Institut Pasteur, Paris, France).

The AP1γ-RBR (AP1γ aa 479–638) was introduced in-frame between GFP and Fyve fingers. pEGFP-Fyve was digested with *Xho*I and *Eco*RI located within the polylinker between GFP and Fyve fingers. The cDNA corresponding to aa 479–638 of AP1γ was amplified by PCR using pP6-AP1γ aa 52–638 as template and the following primers: forward, 5′-gccgtactgagaggatgccagccccc-3′ with a *Xho*I site in the 5′; and reverse, 5′-catgcgaattcttgccaggactgagg-3′ with *Eco*RI in the 5′. The fragment was digested with *Xho*I and *Eco*RI, purified and then ligated into digested pEGFP-Fyve. Rab4b wt, Rab4b Q67L and Rab4b S22N were amplified by PCR by using pEGFP-Rab4b wt/Q67L/S22N as template and a forward primer containing an *Spe*I site in 5′ and a reverse one with a *Pac*I site in order to subclone it in-frame with LexA into the vector pB27 (Hybrigenics Services SAS, Paris, France) predigested with *Spe*I and *Pac*I. The C-terminal deletion of AP1γ (1–488) was performed by introducing a STOP codon at position 488 by site-directed mutagenesis (Cormont et al., 2001). The construction of the N-terminal deletion of AP1γ (1–638) (aa 209–638 and aa 479–638) were performed by subcloning the corresponding fragment amplified by PCR into the *Sma*I site of pAct2. The products of the ligations were digested with *Sma*I before *E. coli* transformation. The orientation of the insert was tested by PCR. pGEX-2T-Rab4b was obtained by subcloning of a PCR-amplified Rab4b fragment in-frame with GST in the *Sma*I site of pGEX-2T. pTrcHis-AP1γ was obtained by subcloning the *Xho*I-*Bam*H1-digested fragment from the pAct2-AP1γ vector into pTrcHis C vector (Invitrogen). All the constructions were verified by sequencing (GATC Biotech SARL, Mulhouse, France).

siRNA

The double-strand siRNAs targeting Rab4b and Rabip4 were synthesised by Eurogentec (Seraing, Belgium). The sequences were as follows: Rab4b forward, CAGGACUCCAACCACACAAdTdT; Rab4b reverse, UUGUGUGGUUGG-AGUCCUGdTdT. siRNA against AP1γ was from Thermo Scientific Dharmacon (On-target plus SMART pool). We used as control siRNA the negative control from Eurogentec or the negative control from Dharmacon. siRNAs were used at a final concentration of 10–20 nM.

Cells

HeLa cells (a gift from T. L. Cover, Vanderbilt, TN) were cultured and transfected as described (Monzo et al., 2005). HeLa cells stably expressing GFP-Rab4b, HA-Rab4b or GFP-Rab4a were selected with geneticin after transfection with pEGFP-Rab4b, pEGFP-Rab4a or pCDNA3-HA-Rab4b, respectively, and maintained in culture in the presence of antibiotics. HEK293 cells were cultured and transfected as described previously (Murdaca et al., 2004).

Yeast two-hybrid screening and interaction measurement

Yeast two-hybrid screening was performed by Hybrigenics Services SAS (Paris, France) by using pB27-Rab4bQ67L as the bait and the human placenta_24 prey library. For interaction measurements, the yeast reporter strain L40 was co-transformed with a pB27–pLex fusion protein vector and pACT2–pP6 fusion protein using a lithium acetate base method and grown on synthetic medium lacking leucine and tryptophan. Induction of the reporter gene *lacZ* was determined using X-gal as substrate (Cormont et al., 2001).

Pull-down experiments

GST-Rab4b or GST was purified as described previously (Cormont et al., 2003). His-AP1γ was purified from *E. coli* transformed with pTrcHis-AP1γ and cultured overnight with 100 μM IPTG. Lysate was loaded on Pro-Bound resin (Invitrogen). After washing, the bound proteins were eluted by increasing the concentration of imidazol (15 mM, 50 mM, 100 mM, 200 mM). The fractions containing His-AP1γ were pooled and dialysed against 25 mM HEPES, pH 7.8, containing 100 mM NaCl. His-AP1γ was enriched among the bacterial proteins but other bacterial proteins that bound the resin were co-purified. The pull-down assay was performed as described (Cormont et al., 2003) except that the glutathione-Sepharose beads were washed in the presence of 0.05% Triton X-100. Proteins within the gel were coloured using InstantBlue (Expedeon) and image were captured with a FujiLAS 3000 in the digitised mode.

Transmission electron microscopy

Cells were fixed with 4% paraformaldehyde in 0.1 M phosphate buffer (PB, pH 7.4) for 2 hours and were processed for ultracryomicrotomy according to a modified Tokuyasu method (Tokuyasu, 1973). Cell suspension was spun down in 10% gelatin. After immersion in 2.3 M sucrose in PB overnight at 4°C, the samples were frozen in liquid nitrogen. 70 nm ultrathin cryosections were prepared with an ultracryomicrotome (Leica EMFCS, Austria) and mounted on formvar-coated nickel grids (Electron Microscopy Sciences, Fort Washington, PA). Immunolabelled cells on grids were processed with an automated immunogold labelling system (Leica EM IGL). The grids were incubated successively in: (1) PBS containing 50 mM NH_4Cl in PBS with 1% BSA; (2) antibodies incubated in PBS with 1% BSA for 1 hour; (3) PBS with 0.1% BSA for gold particle-conjugated secondary antibodies; (4) PBS with 0.1% BSA; (5) PBS alone. The samples were fixed for 10 minutes with 1% glutaraldehyde, rinsed in distilled water and contrasted with 1.8% methylcellulose and 0.3% uranyl acetate on ice. After air drying, sections were examined under a JEOL 1400 transmission electron microscope.

Confocal immunofluorescence microscopy

HeLa cells grown on glass coverslips were fixed in 4% paraformaldehyde and then incubated in 10 mM NH_4Cl. They were permeabilised with PBS containing 1% BSA, 1% SVF and 0.05% saponin or 0.1% Triton X-100. They were then incubated with primary antibodies, washed, and incubated with fluorochrome-coupled secondary antibodies (Alexa Fluor 488, Texas Red or Cy5). After

washing, coverslips were mounted on slides using Mowiol 4-88 in a glycerol-base mounting medium. Confocal analysis was performed with a LSM510META confocal microscope with a PL APO 63× 1.40 NA objective (Carl Zeiss SAS, Gôttingen, Germany) available at the Ibisa-labelled MICA platform of the institute by sequential excitation at 488 nm, 568 nm and 647 nm. Image processing was performed with ImageJ (http://rsb.info.nih.gov/ij/) or Volocity 5.0 (PerkinElmer). Finally, images were merged and figures created with Photoshop (Adobe Systems, Mountain View, CA). The quantification of iTf intensity was performed on 3D images obtained from ten confocal sections for ten fields using Volocity 5.0 software (Perkin Elmer). The same threshold was applied on each 3D image and values were normalised by the number of cells. One image in the control condition at time 0 was arbitrary taken to 1 and the other results were expressed relative to this one.

Tf binding and recycling assays

Cells were serum-deprived for 1 hour before the experiments. The amount of TfR at the plasma membrane was measured by saturation binding of HRP-coupled Tf at 4℃ for 2 hours. Non-specific binding was determined in the presence of an excess of Holo-Tf and represents less than 10% of the total binding. At the end of the incubation, cells were washed twice in PBS with 2% BSA and three times in PBS. The amount of HRP was determined by quantifying the amount of HRP-Tf remaining associated with the cells using fast o-phenylenediamine dihydrochloride (OPD) tablet sets (Sigma-Aldrich). The amount of TfRs at the cell surface was determined by Scatchard analysis of bound HRP-Tf (total binding minus non-specific binding). Results were normalised to the amount of protein determined with the Pierce BCA Protein Assay kit (Thermo Scientific, Rockford, IL).

Internalisation was measured by incubating cells for increasing period of time with HRP-Tf at 37℃. After this, cells were incubated at 4℃ for 2 minutes in acidic buffer (50 mM glycine, 100 mM NaCl, pH 3.0) and washed three times in PBS. Cells were permeabilised with 0.5% Triton X-100 and intracellular HRP-Tf was quantified as above.

Internalisation/recycling assay was performed as described previously (Montagnac et al., 2011). Cells grown on coverslips were incubated at 4℃ with 10 µg/ml of Alexa-Fluor-488-Tf (Invitrogen) for 1 hour. After washing in ice-cold PBS with 1% BSA, coverslips were reincubated at 37℃ in serum-free culture medium complemented with an excess of Holo-Tf during increasing period of times. Cells were then incubated at 4℃ for 2 minutes in acidic buffer and three times with PBS. Cells were fixed in 2% paraformaldehyde and detached from the coverslip using PBS with 20 mM EDTA. The amount of TfR at the plasma membrane was measured by fixing the cells before shifting them at 37℃ and normalised to the cell-associated Alexa-Fluor-488-Tf amount at each time point of the assay. The amount of cell-associated Alexa-Fluor-488-Tf was determined on a MACSQuant analysis system (Miltenyi Biotec SAS, Paris, France). 10 000 cells were analysed. Background fluorescence was measured from acid-washed cells just after the binding step and the value was subtracted from all time points. Statistical analyses were performed using paired Student's *t*-test.

Co-immunoprecipitation

Cells expressing HA-Rab4b or not were washed and solubilised in Tris-HCl, pH 7.4, containing 1% Triton X-100, 10 mM EDTA, 137 mM NaCl and protease inhibitors (Complete, Roche Diagnostics). Lysates (500 µg of protein) were incubated with protein-G-Sepharose beads pre-incubated with 4 µg of antibodies (anti-HA or anti-AP1γ). After a night under agitation at 4℃, beads were washed four times with solubilisation buffer and three times in PBS. Dried beads were resuspended in Laemmli buffer and proteins of the immune pellet were analysed by SDS-PAGE followed by western blotting.

Glycerol gradient centrifugation

Subcellular fractionation on glycerol gradients was performed as previously described (Pérez-Victoria et al., 2008).

Acknowledgements

We thank Drs B. Goud, A. Stenmark, S. Giordano, P. Cossard, C. Bucci, J. Salamero, J. Bonifacino for the gift of plasmids. We thank Dr T. Galli for the gift of anti-Vamp3 antibody. We thank Dr Y. Le Marchand-Brustel for critical reading of the manuscript. We thank Dr E. Lemichez and A. Doye for their help for the purification of recombinant proteins.

Author contributions

P.L., L.-G.S., G.J., C.F., P.D. and C.M. performed experiments. C.M. designed the study and the experiments. B.A., T.J.-F. and C.M. interpreted the data and wrote the manuscript.

Funding

Work was supported by INSERM, the University of Nice-Sophia Antipolis and the ANR [grant number ANR-07-BLAN-046] to C.M. Gilleron Jérôme is supported by the Fondation pour la Recherche Médicale (FRM). The Conseil Général des Alpes-Maritimes, The Conseil Régional PACA, the Association pour la Recherche contre le Cancer (ARC) are acknowledged for their financial support of the Ibisa Imaging Platform Mica of the C3M.

Supplementary material available online at
http://jcs.biologists.org/lookup/suppl/doi:10.1242/jcs.130575/-/DC1

References

Bennett, E. M., Lin, S. X., Towler, M. C., Maxfield, F. R. and Brodsky, F. M. (2001). Clathrin hub expression affects early endosome distribution with minimal impact on receptor sorting and recycling. *Mol. Biol. Cell* **12**, 2790-2799.

Bonifacino, J. S. and Traub, L. M. (2003). Signals for sorting of transmembrane proteins to endosomes and lysosomes. *Annu. Rev. Biochem.* **72**, 395-447.

Chen, Y., Wang, Y., Zhang, J., Deng, Y., Jiang, L., Song, E., Wu, X. S., Hammer, J. A., Xu, T. and Lippincott-Schwartz, J. (2012). Rab10 and myosin-Va mediate insulin-stimulated GLUT4 storage vesicle translocation in adipocytes. *J. Cell Biol.* **198**, 545-560.

Cormont, M., Mari, M., Galmiche, A., Hofman, P. and Le Marchand-Brustel, Y. (2001). A FYVE-finger-containing protein, Rabip4, is a Rab4 effector involved in early endosomal traffic. *Proc. Natl. Acad. Sci. USA* **98**, 1637-1642.

Cormont, M., Metón, I., Mari, M., Monzo, P., Keslair, F., Gaskin, C., McGraw, T. E. and Le Marchand-Brustel, Y. (2003). CD2AP/CMS regulates endosome morphology and traffic to the degradative pathway through its interaction with Rab4 and c-Cbl. *Traffic* **4**, 97-112.

Daro, E., van der Sluijs, P., Galli, T. and Mellman, I. (1996). Rab4 and cellubrevin define different early endosome populations on the pathway of transferrin receptor recycling. *Proc. Natl. Acad. Sci. USA* **93**, 9559-9564.

de Wit, H., Lichtenstein, Y., Kelly, R. B., Geuze, H. J., Klumperman, J. and van der Sluijs, P. (2001). Rab4 regulates formation of synaptic-like microvesicles from early endosomes in PC12 cells. *Mol. Biol. Cell* **12**, 3703-3715.

Delevoye, C., Hurbain, I., Tenza, D., Sibarita, J. B., Uzan-Gafsou, S., Ohno, H., Geerts, W. J. C., Verkleij, A. J., Salamero, J., Marks, M. S. et al. (2009). AP-1 and KIF13A coordinate endosomal sorting and positioning during melanosome biogenesis. *J. Cell Biol.* **187**, 247-264.

Deneka, M., Neeft, M., Popa, I., van Oort, M., Sprong, H., Oorschot, V., Klumperman, J., Schu, P. and van der Sluijs, P. (2003). Rabaptin-5alpha/rabaptin-4 serves as a linker between rab4 and gamma(1)-adaptin in membrane recycling from endosomes. *EMBO J.* **22**, 2645-2657.

Eggers, C. T., Schafer, J. C., Goldenring, J. R. and Taylor, S. S. (2009). D-AKAP2 interacts with Rab4 and Rab11 through its RGS domains and regulates transferrin receptor recycling. *J. Biol. Chem.* **284**, 32869-32880.

Fields, I. C., King, S. M., Shteyn, E., Kang, R. S. and Fölsch, H. (2010). Phosphatidylinositol 3,4,5-trisphosphate localization in recycling endosomes is necessary for AP-1B-dependent sorting in polarized epithelial cells. *Mol. Biol. Cell* **21**, 95-105.

Futter, C. E., Gibson, A., Allchin, E. H., Maxwell, S., Ruddock, L. J., Odorizzi, G., Domingo, D., Trowbridge, I. S. and Hopkins, C. R. (1998). In polarized MDCK cells basolateral vesicles arise from clathrin-gamma-adaptin-coated domains on endosomal tubules. *J. Cell Biol.* **141**, 611-623.

Galvez, T., Gilleron, J., Zerial, M. and O'Sullivan, G. A. (2012). SnapShot: Mammalian Rab proteins in endocytic trafficking. *Cell* **151**, 234-234, e2.

Gaullier, J. M., Simonsen, A., D'Arrigo, A., Bremnes, B., Stenmark, H. and Aasland, R. (1998). FYVE fingers bind PtdIns(3)P. *Nature* **394**, 432-433.

Goueli, B. S., Powell, M. B., Finger, E. C. and Pfeffer, S. R. (2012). TBC1D16 is a Rab4A GTPase activating protein that regulates receptor recycling and EGF receptor signaling. *Proc. Natl. Acad. Sci. USA* **109**, 15787-15792.

Grant, B. D. and Donaldson, J. G. (2009). Pathways and mechanisms of endocytic recycling. *Nat. Rev. Mol. Cell Biol.* **10**, 597-608.

Gravotta, D., Carvajal-Gonzalez, J. M., Mattera, R., Deborde, S., Banfelder, J. R., Bonifacino, J. S. and Rodriguez-Boulan, E. (2012). The clathrin adaptor AP-1A mediates basolateral polarity. *Dev. Cell* **22**, 811-823.

Gurkan, C., Lapp, H., Alory, C., Su, A. I., Hogenesch, J. B. and Balch, W. E. (2005). Large-scale profiling of Rab GTPase trafficking networks: the membrome. *Mol. Biol. Cell* **16**, 3847-3864.

Hoogenraad, C. C., Popa, I., Futai, K., Martinez-Sanchez, E., Wulf, P. S., van Vlijmen, T., Dortland, B. R., Oorschot, V., Govers, R., Monti, M. et al. (2010). Neuron specific Rab4 effector GRASP-1 coordinates membrane specialization and maturation of recycling endosomes. *PLoS Biol.* **8**, e1000283.

Johannes, L. and Popoff, V. (2008). Tracing the retrograde route in protein trafficking. *Cell* **135**, 1175-1187.

Kachhap, S. K., Faith, D., Qian, D. Z., Shabbeer, S., Galloway, N. L., Pili, R., Denmeade, S. R., DeMarzo, A. M. and Carducci, M. A. (2007). The N-Myc down regulated Gene1 (NDRG1) Is a Rab4a effector involved in vesicular recycling of E-cadherin. *PLoS ONE* **2**, e844.

Kaddai, V., Gonzalez, T., Keslair, F., Grémeaux, T., Bonnafous, S., Gugenheim, J., Tran, A., Gual, P., Le Marchand-Brustel, Y. and Cormont, M. (2009). Rab4b is a small GTPase involved in the control of the glucose transporter GLUT4 localization in adipocyte. *PLoS ONE* **4**, e5257.

Kang, H. J., Voleti, B., Hajszan, T., Rajkowska, G., Stockmeier, C. A., Licznerski, P., Lepack, A., Majik, M. S., Jeong, L. S., Banasr, M. et al. (2012). Decreased expression of synapse-related genes and loss of synapses in major depressive disorder. *Nat. Med.* **18**, 1413-1417.

Krawczyk, M., Leimgruber, E., Seguín-Estévez, Q., Dunand-Sauthier, I., Barras, E. and Reith, W. (2007). Expression of RAB4B, a protein governing endocytic recycling, is co-regulated with MHC class II genes. *Nucleic Acids Res.* **35**, 595-605.

Mallard, F., Antony, C., Tenza, D., Salamero, J., Goud, B. and Johannes, L. (1998). Direct pathway from early/recycling endosomes to the Golgi apparatus revealed through the study of shiga toxin B-fragment transport. *J. Cell Biol.* **143**, 973-990.

Mari, M., Monzo, P., Kaddai, V., Keslair, F., Gonzalez, T., Le Marchand-Brustel, Y. and Cormont, M. (2006). The Rab4 effector Rabip4 plays a role in the endocytotic trafficking of Glut 4 in 3T3-L1 adipocytes. *J. Cell Sci.* **119**, 1297-1306.

Maxfield, F. R. and McGraw, T. E. (2004). Endocytic recycling. *Nat. Rev. Mol. Cell Biol.* **5**, 121-132.

McCaffrey, M. W., Bielli, A., Cantalupo, G., Mora, S., Roberti, V., Santillo, M., Drummond, F. and Bucci, C. (2001). Rab4 affects both recycling and degradative endosomal trafficking. *FEBS Lett.* **495**, 21-30.

Montagnac, G., de Forges, H., Smythe, E., Gueudry, C., Romao, M., Salamero, J. and Chavrier, P. (2011). Decoupling of activation and effector binding underlies ARF6 priming of fast endocytic recycling. *Curr. Biol.* **21**, 574-579.

Monzo, P., Gauthier, N. C., Keslair, F., Loubat, A., Field, C. M., Le Marchand-Brustel, Y. and Cormont, M. (2005). Clues to CD2-associated protein involvement in cytokinesis. *Mol. Biol. Cell* **16**, 2891-2902.

Murdaca, J., Treins, C., Monthouël-Kartmann, M. N., Pontier-Bres, R., Kumar, S., Van Obberghen, E. and Giorgetti-Peraldi, S. (2004). Grb10 prevents Nedd4-mediated vascular endothelial growth factor receptor-2 degradation. *J. Biol. Chem.* **279**, 26754-26761.

Ohno, H., Tomemori, T., Nakatsu, F., Okazaki, Y., Aguilar, R. C., Foelsch, H., Mellman, I., Saito, T., Shirasawa, T. and Bonifacino, J. S. (1999). μ1B, a novel adaptor medium chain expressed in polarized epithelial cells. *FEBS Lett.* **449**, 215-220.

Pagano, A., Crottet, P., Prescianotto-Baschong, C. and Spiess, M. (2004). In vitro formation of recycling vesicles from endosomes requires adaptor protein-1/clathrin and is regulated by rab4 and the connector rabaptin-5. *Mol. Biol. Cell* **15**, 4990-5000.

Pereira-Leal, J. B. and Seabra, M. C. (2001). Evolution of the Rab family of small GTP-binding proteins. *J. Mol. Biol.* **313**, 889-901.

Pérez-Victoria, F. J., Mardones, G. A. and Bonifacino, J. S. (2008). Requirement of the human GARP complex for mannose 6-phosphate-receptor-dependent sorting of cathepsin D to lysosomes. *Mol. Biol. Cell* **19**, 2350-2362.

Pfeffer, S. R. (2011). Entry at the trans-face of the Golgi. *Cold Spring Harb. Perspect. Biol.* **3**, a005272.

Poteryaev, D., Datta, S., Ackema, K., Zerial, M. and Spang, A. (2010). Identification of the switch in early-to-late endosome transition. *Cell* **141**, 497-508.

Raiborg, C., Bache, K. G., Gillooly, D. J., Madshus, I. H., Stang, E. and Stenmark, H. (2002). Hrs sorts ubiquitinated proteins into clathrin-coated microdomains of early endosomes. *Nat. Cell Biol.* **4**, 394-398.

Rink, J., Ghigo, E., Kalaidzidis, Y. and Zerial, M. (2005). Rab conversion as a mechanism of progression from early to late endosomes. *Cell* **122**, 735-749.

Robinson, M. S. and Bonifacino, J. S. (2001). Adaptor-related proteins. *Curr. Opin. Cell Biol.* **13**, 444-453.

Sachse, M., Urbé, S., Oorschot, V., Strous, G. J. and Klumperman, J. (2002). Bilayered clathrin coats on endosomal vacuoles are involved in protein sorting toward lysosomes. *Mol. Biol. Cell* **13**, 1313-1328.

Sönnichsen, B., De Renzis, S., Nielsen, E., Rietdorf, J. and Zerial, M. (2000). Distinct membrane domains on endosomes in the recycling pathway visualized by multicolor imaging of Rab4, Rab5, and Rab11. *J. Cell Biol.* **149**, 901-914.

Stenmark, H. (2012). The Rabs: a family at the root of metazoan evolution. *BMC Biol.* **10**, 68.

Stoorvogel, W., Oorschot, V. and Geuze, H. J. (1996). A novel class of clathrin-coated vesicles budding from endosomes. *J. Cell Biol.* **132**, 21-33.

Tokuyasu, K. T. (1973). A technique for ultracryotomy of cell suspensions and tissues. *J. Cell Biol.* **57**, 551-565.

van der Sluijs, P., Hull, M., Webster, P., Mâle, P., Goud, B. and Mellman, I. (1992). The small GTP-binding protein rab4 controls an early sorting event on the endocytic pathway. *Cell* **70**, 729-740.

van Weering, J. R., Verkade, P. and Cullen, P. J. (2012). SNX-BAR-mediated endosome tubulation is co-ordinated with endosome maturation. *Traffic* **13**, 94-107.